

# Integrated Attitude Determination and Control System via Magnetic Measurements and Actuation

MOHAMMAD ABDELRAHMAN AND SANG-YOUNG PARK

Astrodynamics and Control Lab (ACL), Department of Astronomy and Space Science  
Yonsei University

120-749, Seoul, Republic of KOREA

[m\\_abdelrahman@galaxy.yonsei.ac.kr](mailto:m_abdelrahman@galaxy.yonsei.ac.kr), [spark@galaxy.yonsei.ac.kr](mailto:spark@galaxy.yonsei.ac.kr)

*Abstract:* - A nonlinear control scheme using a Modified State-Dependent Riccati Equation MSDRE has been developed through a pseudo-linearization of spacecraft augmented dynamics and kinematics. The full-state knowledge, required for the control loop is provided through a generalized algorithm for spacecraft three-axis attitude and rate estimation based on the utilization of magnetometer measurements and their time derivatives, while the control torque is generated via magnetorquers. The resulted attitude determination and control system has shown the capability of estimating the attitude better than 5 deg and rate of order 0.03 deg/sec in addition to maintain the pointing accuracy within 5 deg in each axis with pointing stability of less than 0.05 deg/sec.

*Key-Words:* - Attitude Control, Attitude Estimation, Magnetometer, Magnetorquers, Modified Riccati Equation, Nonlinear Control.

## 1 Introduction

The aim of this paper is to develop a low cost three-axis Attitude Determination and Control System ADCS to fulfill spacecraft mission requirements during low accuracy modes which are the most frequent modes during mission life time. The current work introduces a generalized nonlinear control scheme using a Modified State-Dependent Riccati Equation MSDRE. The system dynamics equation is represented by the spacecraft nonlinear dynamics with momentum bias including gravity gradient, aerodynamic, and magnetic residual torques. Then, the quaternion kinematics is augmented with spacecraft dynamics to represent the overall process dynamics. A pseudo-linear formulation of the augmented system is developed while a MSDRE controller derived to solve a trajectory tracking/model following problem. The derivatives of the state dependent matrix w.r.t the states are taken into account through the development of the final MSDRE controller such that an optimal control signal is obtained rather than producing a suboptimal controller when these derivatives are ignored. To obtain the optimum control signal full-state knowledge is required, so attitude and rate filter is integrated to the control loop. The proposed filter is previously developed by the authors for spacecraft three-axis attitude and rate estimation utilizing magnetometer measurements only [7]. The global asymptotic stability of the controller is investigated by applying Lyapunov theorem, and concluded by introducing stability regimes for the overall system which verify the stability conditions of the controller and the required accuracy of the filter. To test the developed ADCS, EgyptSat-1, launched in the last April, is used as a real test

case. Basically, the ADCS has been tested to control the satellite and estimate the attitude and rates during detumbling and standby modes where the magnetometer measurements and magnetorquers only can fulfill the mission attitude and rate accuracy requirements for these two modes. The next section describes briefly the statement of the problem then the MSDRE controller is developed and adopted for tracking problem. Through the fourth section the pseudo-linear representation of the system is derived and the stability issues are introduced. Before the simulation section, the state estimator design appears and discussed. Finally, the paper is concluded by testing the proposed ADCS via simulations.

## 2 Statement of the Problem

Consider the nonlinear system

$$\dot{x} = f(x, t) + v_x(t) \quad (1)$$

we will try to control this system such that its output is expressed as

$$y = cx \quad (2)$$

with the availability of a set of measurements

$$z = h(x, t) + v_z(t) \quad (3)$$

where  $v_x(t)$  and  $v_z(t)$  are random zero-mean processes described by the process and measurement noise matrices  $Q_f = E(v_x v_x^T)$  and  $R_f = E(v_z v_z^T)$ . Now the task is to design a controller such that the system tracks a specified reference trajectory while a state estimator shall be plugged in to provide the necessary states to drive the controller. The reference trajectory is given by

$$\dot{\chi} = F\chi \quad (4)$$

$$y_{ref} = C\chi \quad (5)$$

the pair  $[F, C]$  is supposed to be completely observable.

### 3 The MSDRE Controller Design

The control approach will be based on using the Differential State Dependent Riccati Equation DSDRE to solve tracking/model following problem. Let's start by converting the nonlinear dynamics into a pseudo-linear system

$$\dot{x} = A(x)x + Gu \quad (6)$$

where  $u$  is the control signal. Note the process noise part is dropped in the controller design and it will be included through the estimator development. A new dynamic system can be derived by augmenting the pseudo-linear system with the reference trajectory model such that

$$\dot{\tilde{x}} = \tilde{A}(\tilde{x}, t)\tilde{x} + \tilde{G}u \quad (7)$$

where  $\tilde{x} = \begin{bmatrix} x \\ \chi \end{bmatrix}$ ,  $\tilde{A} = \begin{bmatrix} A & 0 \\ 0 & F \end{bmatrix}$  and  $\tilde{G} = \begin{bmatrix} G \\ 0 \end{bmatrix}$ . Then a quadratic cost function  $J$  is defined as

$$J = \frac{1}{2} \int_{t_0}^{t_f} [\tilde{x}^T \tilde{Q} \tilde{x} + u^T R u] dt \quad (8)$$

where  $\tilde{Q} = \begin{bmatrix} Q & -QC \\ -C^T Q & C^T Q C \end{bmatrix}$  and nonnegative definite symmetric, while  $R$  is positive definite symmetric. From the above, a generalized Riccati equation can be derived.

$$-\dot{\tilde{P}} = [\tilde{P}\tilde{A} + \tilde{A}^T\tilde{P} - \tilde{P}\tilde{G}R^{-1}\tilde{G}^T\tilde{P} + \tilde{Q}] + \left[ \left( \frac{\partial \tilde{A}}{\partial \tilde{x}_i} \tilde{x} \right)^T \tilde{P} + \left( \frac{\partial \tilde{G}}{\partial x_i} u \right)^T \tilde{P} - \tilde{P}\tilde{G}R^{-1} \left( \frac{\partial \tilde{G}}{\partial u} u \right)^T \tilde{P} \right] \quad (9)$$

The first part of this equation is the well known state-dependent Riccati equation, and the second part is due to the nonlinearity of the system. Neglecting the second part leads to only a suboptimal control. Through this work the matrix  $\tilde{G}$  is only function of time, so the modified state-dependent Riccati equation MSDRE for optimal control is

$$-\dot{\tilde{P}} = \tilde{P}\tilde{A} + \tilde{A}^T\tilde{P} - \tilde{P}\tilde{G}R^{-1}\tilde{G}^T\tilde{P} + \left( \frac{\partial \tilde{A}}{\partial \tilde{x}_i} \tilde{x} \right)^T \tilde{P} + \tilde{Q} \quad (10)$$

with a boundary condition,  $\tilde{P}(t_f) = 0$ . This gives immediately the optimal control  $u$

$$u = -R^{-1}\tilde{G}^T\tilde{P}\tilde{x} \quad (11)$$

The matrix  $\tilde{P}$  can be partitioned as,

$$\tilde{P} = \begin{bmatrix} P & P_{12} \\ P_{21} & P_{22} \end{bmatrix} \quad (12)$$

this gives the optimal control as follows

$$u = Kx + K_\chi \chi \quad (13)$$

where

$$K = -R^{-1}G^T P \quad (14)$$

and

$$K_\chi = -R^{-1}G^T P_{12} \quad (15)$$

Figure 1 shows the augmented system controlled by use of linear state-variable feedback, as for a standard regulator. The modified Riccati equation becomes

$$-\dot{P} = PA + A^T P - PGR^{-1}G^T P + \left( \frac{\partial A}{\partial x_i} x \right)^T P + Q \quad (16)$$

The reference trajectory  $y_{ref}$  is usually given in a form of

points calculated offline and can be interpolated with time so, let's try to avoid the pair  $[F, C]$  in the Riccati equations. Define a new vector  $b_{ext}$ , where  $ext$  stands for an external control signal as we will see

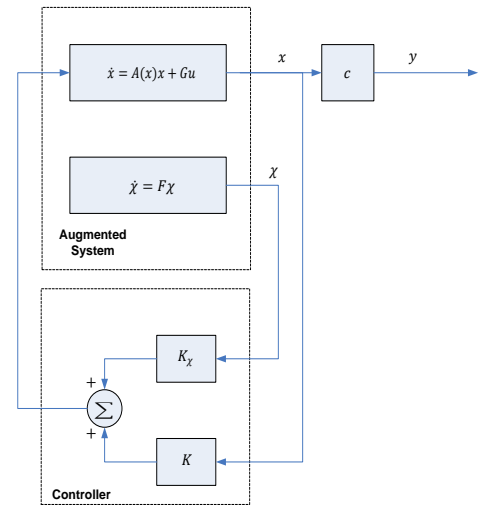


Fig. 1 Augmented System Control [2]

$$b_{ext} = P_{12}\chi \quad (17)$$

$$-\dot{b}_{ext} = -\dot{P}_{12}\chi - P_{12}\dot{\chi} \quad (18)$$

Using reference trajectory model in Eqs (4) and (5) leads to,

$$-\dot{b}_{ext} = \left[ A^T + \left( \frac{\partial A}{\partial x_i} x \right)^T - PGR^{-1}G^T \right] b_{ext} - Qy_{ref} \quad (19)$$

Similar treatment can be applied for  $P_{21}$  and  $P_{22}$  defining two new vectors  $c_{ext}$  and  $d_{ext}$  as follows

$$c_{ext} = P_{21}^T \chi \quad (20)$$

and

$$d_{ext} = \chi^T P_{22} \chi \quad (21)$$

Then the differential equations of  $c_{ext}$  and  $d_{ext}$  can be written as

$$-\dot{c}_{ext} = [A - GR^{-1}G^T P]^T c_{ext} - Qy_{ref} \quad (22)$$

and

$$\dot{d}_{ext} = c_{ext}^T GR^{-1}G^T b_{ext} - y_{ref}^T Qy_{ref} \quad (23)$$

Finally the optimal control can be rewritten as

$$u = Kx + u_{ext} \quad (24)$$

where

$$u_{ext} = -R^{-1}G^T b_{ext} \quad (25)$$

represents the external control signal Fig.2. To summarize, we need to integrate the modified Riccati equations for  $P$  and  $b_{ext}$ , then the optimal control signal can be obtained. The boundary conditions for the MSDRE are  $P(t_f) = 0$  and  $b_{ext}(t_f) = 0$ .

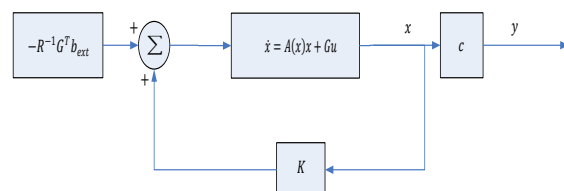


Fig. 2 Optimal Trajectory Control [2]

## 4 Spacecraft Attitude Maneuver Using MSDRE

This section provides a background about the spacecraft dynamics and kinematics modelling with proposed disturbances, and then a pseudo-linear representation for this model is adopted such that the application of the MSDRE scheme can be implemented.

### 4.1 Spacecraft Attitude Dynamics

The attitude dynamics of a rigid spacecraft can be expressed by the well-known Euler's equation in presence of momentum exchange devices and given

$$\dot{\omega} = -I^{-1}[\omega \times (I\omega + h)] + I^{-1}(T - \dot{h}) \quad (26)$$

The torque  $T$  is the total torque vector exerted on the spacecraft which includes gravity gradient torque

$$T_{gg} = \frac{3\mu}{|R_S|^3} [\hat{R}_S \times (I\hat{R}_S)] \quad (27)$$

where  $R_S$  is the position vector, and  $\mu$  is the Earth's gravitational constant. Then the aerodynamic torque

$$T_{aero} = \frac{1}{2} C_d \rho |V_{rel}|^2 \sum_{i=1}^n (\hat{N}_i \cdot \hat{V}_{rel}) (\hat{V}_{rel} \times r_i) A_i \quad (28)$$

The summation is taken over  $n$  surfaces of the spacecraft with area  $A_i$  and unit outward normal vector  $\hat{N}_i$ . The parameter  $C_d$  is the drag coefficient and  $\rho$  is the atmosphere density. The velocity vector relative to the rotating atmosphere is  $V_{rel} = V_S - \omega_{\oplus} \times R_S$ , where  $\omega_{\oplus}$  is the Earth's rotational velocity, and  $V_S$  is the spacecraft velocity. Also, the magnetic disturbance torque

$$T_m = m \times B \quad (29)$$

The spacecraft dipole moment is the vector  $m$  while  $B$  is the Earth's magnetic field. The control strategy is based on using only magnetic torquers in a momentum biased system, so the control torque is given by

$$T_c = M \times B \quad (30)$$

where  $M$  is the dipole moment generated by the magnetic torquers. Let's assume that there is another control signal  $u$  which constructs an orthogonal set with the two vectors  $M$ , and  $B$ , then

$$T_c = -\frac{[B \times][B \times]}{|B|^2} u = \bar{G}u \quad (31)$$

where the anti-symmetric matrix  $[B \times]$  is defined by

$$[B \times] = \begin{bmatrix} 0 & -b_3 & b_2 \\ b_3 & 0 & -b_1 \\ -b_2 & b_1 & 0 \end{bmatrix} \quad (32)$$

Finally, the total torque is  $T = T_{gg} + T_{aero} + T_m + T_c$ . Note all vectors in the previous equations are derived in the spacecraft body frame.

### 4.2 Quaternion Kinematics

The spacecraft attitude is represented through the quaternion, defined by

$$q \equiv \begin{bmatrix} q_4 \\ q_1 \\ q_2 \\ q_3 \end{bmatrix} \quad (33)$$

while the vector part  $q_{13} \equiv [q_1 \ q_2 \ q_3]^T = \hat{n} \sin(\alpha/2)$  and

the scalar part  $q_4 = \cos(\alpha/2)$ . Here  $\hat{n}$  is a unit vector corresponding to the principal axis of rotation and  $\alpha$  is the angle of rotation. The quaternion kinematics is derived through the spacecraft's angular velocity as follows

$$\dot{q} = \frac{1}{2} \Omega(\omega) q = \frac{1}{2} \Xi(q) \omega \quad (34)$$

where  $\Omega(\omega)$  and  $\Xi(q)$  are defined as

$$\Omega(\omega) = \begin{bmatrix} -[\omega \times] & \vdots & \omega \\ \dots & \vdots & \dots \\ -\omega^T & \vdots & 0 \end{bmatrix} \text{ and } \Xi(q) = \begin{bmatrix} q_4 U_{3 \times 3} + [q_{13} \times] \\ \dots \\ -q_{13}^T \end{bmatrix}$$

Here  $U_{3 \times 3}$  is a unit matrix. The quaternion four elements satisfy the following normalization constraint  $q^T q = q_{13}^T q_{13} + q_4^2 = 1$ .

### 4.3 Pseudo-Linear Modelling

Now the task is to derive a pseudo-linear system in the form of Eq.(6) such that the MSDRE control scheme can be applied. Starting with the state vector  $x$  resulting from the augmentation of the spacecraft dynamics with the quaternion kinematics as follows

$$x^T = [\omega \ q]^T \quad (35)$$

The state vector  $x$  describes the spacecraft angular velocity and attitude in the body frame w.r.t the inertial frame. Let's consider the first part of the attitude dynamic equation

$$F_1 = -I^{-1}[\omega \times (I\omega + h)] = \frac{1}{2} \frac{\partial F_1}{\partial \omega} \omega + \frac{1}{2} I^{-1}[h \times] \omega \quad (36)$$

The attitude matrix is given by

$$\Pi = (q_4^2 - q_{13}^T q_{13}) U_{3 \times 3} + 2q_{13} q_{13}^T - 2q_4 [q_{13} \times] \quad (37)$$

and its derivatives w.r.t  $q_i$  are

$$\frac{\partial \Pi}{\partial q_i} = -2q_i U_{3 \times 3} + 2[q_{13} u_i^T + u_i q_{13}^T] - 2q_4 [u_i \times] \quad (38)$$

$u_i$  is  $i^{\text{th}}$  column of the unit matrix  $U$  and  $i = 1 \dots 3$ .

$$\frac{\partial \Pi}{\partial q_4} = 2q_4 U_{3 \times 3} - 2[q_{13} \times] \quad (39)$$

From the above it can be shown that  $\Pi = \frac{1}{2} \sum_{i=1}^4 \frac{\partial \Pi}{\partial q_i} q_i$ . If there is a vector expressed in the inertial frame  $T_I$ , its transformation to body frame  $T_b$  is obtained by

$$T_b = \Pi T_I = \frac{1}{2} \sum_{i=1}^4 \frac{\partial \Pi}{\partial q_i} q_i T_I = \frac{1}{2} \frac{\partial T_b}{\partial q} q \quad (40)$$

Applying this result to the second part of the attitude dynamic equation i.e. torque vectors, leads to

$$T_{gg} = \frac{1}{4} \frac{\partial T_{gg}}{\partial q} q, T_m = \frac{1}{2} \frac{\partial T_m}{\partial q} q, \text{ and } T_{aero} = \frac{1}{4} \frac{\partial T_{aero}}{\partial q} q.$$

Note the Earth's rotation effect is neglected w.r.t spacecraft velocity. Also, the quaternion kinematics can be rewritten as follows:

$$\dot{q} = \frac{1}{2} \left[ \frac{\partial \dot{q}}{\partial \omega} \omega + \frac{\partial \dot{q}}{\partial q} q \right] \quad (41)$$

Now the augmented attitude dynamics and kinematics equations can be expressed in pseudo-linear form

$$\begin{bmatrix} \dot{\omega} \\ \vdots \\ \dot{q} \end{bmatrix} = \frac{1}{2} \begin{bmatrix} \frac{\partial F_1}{\partial \omega} & \vdots & I^{-1} \left( \frac{\partial T_{gg}}{\partial q} + \frac{\partial T_m}{\partial q} + \frac{\partial T_{aero}}{\partial q} \right) \\ \vdots & \vdots & \vdots \\ \frac{\partial \dot{q}}{\partial \omega} & \vdots & \frac{\partial \dot{q}}{\partial q} \\ \vdots & \vdots & \vdots \end{bmatrix} \begin{bmatrix} \omega \\ \vdots \\ q \end{bmatrix} + \begin{bmatrix} I^{-1} \bar{G} \\ \vdots \\ 0 \end{bmatrix} u + \begin{bmatrix} \frac{1}{2} I^{-1} [h \times] & \vdots & -\frac{1}{4} I^{-1} \left( \frac{\partial T_{gg}}{\partial q} + \frac{\partial T_{aero}}{\partial q} \right) \\ \vdots & \vdots & \vdots \\ 0 & \vdots & 0 \end{bmatrix} \begin{bmatrix} \omega \\ \vdots \\ q \end{bmatrix}$$

or

$$\dot{x} = A(x)x + Gu + \Gamma(x)x \quad (42)$$

The effect of the matrix  $\Gamma(x)$  on the system is negligible compared to  $A(x)$  and is proved by simulation as will be presented in the section of simulations results. Consider the augmented system without the control vector

$$\dot{\tilde{x}} = \bar{f}(x, t) = A(x)x \quad (43)$$

simply,  $A(x) = \frac{1}{2} \frac{\partial \bar{f}}{\partial x}$ , where  $\frac{\partial \bar{f}}{\partial x}$  is the Jacobian

$$\frac{\partial \dot{\tilde{x}}}{\partial x_i} = \frac{\partial \bar{f}}{\partial x_i} = \frac{\partial A(x)}{\partial x_i} x + A(x)_i \quad (44)$$

where  $A(x)_i$  is  $i^{\text{th}}$  column of the matrix  $A(x)$ . From the above  $\left( \frac{\partial A(x)}{\partial x_i} x \right) = A(x)$ . The reference trajectory can be obtained by

$$\omega_{ref} = \omega_{ref}^{bo} + \Pi_{ref}^{bo} \omega^{rl} \quad (45)$$

$$q_{ref} = q_{ref}^{bo} \otimes q^{ol} \quad (46)$$

where  $b, o$ , and  $I$  stand for body, orbit, and inertial frames, respectively. Usually the reference trajectory is given in body frame w.r.t orbit frame so the previous relations are used to derive the corresponding reference trajectory in body frame w.r.t inertial frame. Then  $y_{ref}^T = [\omega_{ref} \quad q_{ref}]^T$ . Now, we can apply the MSDRE control scheme to spacecraft attitude tracking using the backward solution of

$$-\dot{P} = PA + 2A^T P - PGR^{-1}G^T P + Q \quad (47)$$

$$-\dot{b}_{ext} = [2A^T - PGR^{-1}G^T]b_{ext} - Qy_{ref} \quad (48)$$

The control gain  $K$ , the external control component  $u_{ext}$ , and the optimal control signal  $u$  are obtained through Eq.(14), Eq.(25), and Eq.(24), respectively.

#### 4.4 Effect of Actuator Saturation

Due to the actuator saturation the optimal dipole moment  $M^*$  resulting from the MSDRE controller should be scaled down keeping its direction as it is. From Fig. 3 the following relation can be obtained

$$M_s^* = \frac{M_{max}}{M_i^*} M^* \quad (49)$$

where  $M_s^*$  is the scaled dipole moment,  $M_{max}$  is the maximum dipole moment of the magnetic torquer, and  $M_i^*$  is the maximum projected dipole moment on  $i$  axis.

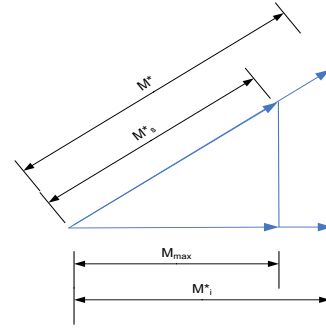


Fig. 3 Schematic Diagram for Scaled Dipole Moment

#### 4.5 Stability of the MSDRE Controller

Based on Lyapunov's method, stability regimes of the MSDRE can be estimated. Choose  $V(\tilde{x}) = \tilde{x}^T \tilde{P} \tilde{x}$  as a Lyapunov function candidate, where  $\tilde{P}$  is the positive definite solution of the modified Riccati equation Eq.(10). Rewriting

$$V = x^T P x + x^T b_{ext} + c_{ext}^T x + d_{ext} \quad (50)$$

then the time derivative becomes

$$\dot{V} = \dot{x}^T P x + x^T \dot{P} x + x^T P \dot{x} + \dot{x}^T b_{ext} + x^T \dot{b}_{ext} + \dot{c}_{ext}^T x + c_{ext}^T \dot{x} + \dot{d}_{ext} \quad (51)$$

sub., with Eq.(6) where  $u = -R^{-1}G^T P x - R^{-1}G^T b_{ext}$  and using the modified Riccati equations

$$\begin{aligned} \dot{V} = & -[\eta^T R \eta + \lambda^T R^{-1} \lambda + x^T Q x + y_{ref}^T Q y_{ref}] \\ & - [2\lambda^T \eta + x^T A^T (P x + b_{ext})] \\ & + [y_{ref}^T Q x + x^T Q y_{ref}] \end{aligned} \quad (52)$$

where  $\eta = R^{-1}G^T P x$  and  $\lambda = G^T b_{ext}$ . Since  $Q$  and  $R$  are positive definite matrices then the first part is negative, also the last part is small and can be neglected specially when  $y_{ref}^T = [0_{6 \times 1} \quad 1]^T$  and the last term of the  $Q$  matrix is chosen to be relatively small. Then regions should be estimated to ensure negative values of the second term and hence the stability of the system. To estimate the stability regions of the candidate MSDRE controller, uniformly random distributed initial conditions  $\Theta$  and  $\Omega$  on the intervals  $\pm \Theta^*$  deg and  $\pm \Omega^*$  deg/s for each axis, are generated and the following conditions are investigated:

$$V(x) > 0 \text{ and } \dot{V}(x) < 0 \quad (53)$$

### 5 State Estimator Design

The well known extended Kalman filter EKF is used through this work as a state estimator to provide the MSDRE controller with the necessary states required to drive the controller.

#### 5.1 Filter Process Model

The spacecraft dynamics and kinematics, given in Eqs. (26) and (34) are augmented to represent the system process model. Also, the spacecraft residual dipole and the drag coefficient are added to the state vector for more filter robustness.

$$\begin{bmatrix} \dot{\omega} \\ \dots \\ \dot{q} \\ \dots \\ \dot{m} \\ \dots \\ \dot{C}_d \end{bmatrix} = \begin{bmatrix} -I^{-1}[\omega \times (I\omega + h)] + I^{-1}(T - \dot{h}) \\ \dots \\ \frac{1}{2}\Xi(q)\omega \\ \dots \\ 0 \\ \dots \\ 0 \end{bmatrix} + \begin{bmatrix} v_\omega \\ \dots \\ 0 \\ \dots \\ v_m \\ \dots \\ v_c \end{bmatrix} \quad (54)$$

$$\dot{x} = f(x, t) + v_x(t)$$

The state vector  $x$  is eleven-dimensional, defined as

$$x^T = [\omega \quad q \quad m \quad C_d]^T \quad (55)$$

## 5.2 Filter Measurement Model

The measurement equation, required for the application of the extended Kalman filtering, is derived from vector kinematics and considered to be a nonlinear function of the states according to

$$\begin{bmatrix} B_b \\ \dots \\ \dot{B}_b \end{bmatrix} = \begin{bmatrix} \Pi B_l \\ \dots \\ \Pi \dot{B}_l - \omega \times (\Pi B_l) \end{bmatrix} + \begin{bmatrix} v_B \\ \dots \\ v_{\dot{B}} \end{bmatrix} \quad (56)$$

$$z = h(x, t) + v_z(t)$$

where  $B_l$  is a vector of some reference such as the position vector to the Sun, to a star or the Earth's magnetic field vector in a reference coordinate system, and  $B_b$  is the corresponding measured vector in the spacecraft body frame. Only magnetometer measurements and its time derivatives are considered through this work. The prediction of the state estimates and covariance are accomplished by

$$\hat{x}_k^- = \int_0^{\Delta t} f(x, \tau) dt \quad (57)$$

$$P_{f_k}^- = \Phi_k P_{f_{k-1}}^- \Phi_k^T + Q_{f_k} \quad (58)$$

where  $\Phi \approx U + \frac{\partial f}{\partial x} \Delta t$  is the state transition matrix and  $P_f$  is the error covariance matrix. It obviously can be shown that the derivatives needed for the Jacobian  $\frac{\partial f}{\partial x}$  are already included in the state-dependent matrix  $A(x)$ . Only it is needed to calculate the derivative of the control torque w.r.t the states which simply can be given as  $\frac{\partial T_c}{\partial x} = GK$ . Note an accurate integration method should be used to perform the state propagation. The discrete process covariance  $Q_{f_k}$  is computed according to  $Q_{f_k} = \int_0^{\Delta t} \Phi(\tau) Q_f \Phi^T(\tau) dt$ . A closed form solution can be obtained as

$$\begin{aligned} \bar{q}_{ii_f} &= q_{i_f} \Delta t (1 + a_{ii} \Delta t) + \sum_{j=1}^n \frac{q_{j_f} a_{ij}^2 \Delta t^3}{3} \\ \bar{q}_{ij_f} &= q_{i_f} a_{ji} \Delta t^2 \left( \frac{1}{2} + a_{ii} \frac{\Delta t}{3} \right) \\ &+ q_{j_f} a_{ij} \Delta t^2 \left( \frac{1}{2} + a_{jj} \frac{\Delta t}{3} \right) + \sum_{\substack{l=1 \\ l \neq i \\ l \neq j}}^n \frac{q_{l_f} a_{il} a_{jl} \Delta t^3}{3} \end{aligned} \quad (59)$$

where  $i, j = 1 \dots N$ , and  $n = N - i$ . Here  $N$  is the no. of states,  $q_{i_f}$  and  $\bar{q}_{ij_f}$  are the elements of matrices  $Q_f$  and

$Q_{f_k}$  respectively ( $Q_f$  is assumed to be diagonal) while  $a_{ij}$  is the elements of the Jacobian matrix  $\frac{\partial f}{\partial x}$ . Finally, as with the basic discrete Kalman filter, the measurement update equations correct the state and covariance estimates with the measurements  $z_k$  as follows

$$K_{f_k} = P_{f_k}^- H_k^T (H_k P_{f_k}^- H_k^T + R_{f_k})^{-1} \quad (60)$$

$$\hat{x}_k = \hat{x}_k^- + K_{f_k} [z_k - h(\hat{x}_k^-)] \quad (61)$$

$$P_{f_k} = (U - K_{f_k} H_k) P_{f_k}^- (U - K_{f_k} H_k)^T + K_{f_k} R_{f_k} K_{f_k}^T \quad (62)$$

where  $H = \left. \frac{\partial h(x, t)}{\partial x} \right|_{x=\hat{x}}$  and  $K_{f_k}$  is the Kaman gain.

## 6 Simulation Results

To test the developed ADCS, EgyptSat-1, injected in sun-synchronous low Earth orbit is used as a real test case. The initial control strategy of EgyptSat-1 was to utilize only the magnetorquers to detumble the spacecraft after separation and then to use the magnetometer reading to estimate the attitude and rates during the standby/stabilization mode. Unfortunately, during the commissioning phase the reaction wheels had been used in additions to magnetorquers to detumble the spacecraft in order to maintain the power profile of the spacecraft, since it was found that using only magnetorquers would not detumble the spacecraft in the proper time. Also, the fiber gyros onboard had to be used for rate measurements and a strap down scheme was used for obtaining the attitude. The proposed controller/estimator design is utilized through both detumbling and standby/stabilization modes using only magnetorquers and magnetometer readings to meet the ADCS requirements, summarized by depressing the total angular velocity after separation to less than  $0.1 \text{ deg/sec}$  in one orbit and half. Then to bring the spacecraft to stabilization (Earth pointing) mode in no more than three orbits due to the spacecraft power profile. Also, to maintain the pointing accuracy during stabilization mode within  $5 \text{ deg}$  and rate less than  $0.05 \text{ deg/sec}$  in each axis. Finally, to achieve attitude determination accuracy better than  $5 \text{ deg}$  and rate of  $0.03 \text{ deg/sec}$  during the same mode. Before the discussion of the simulations results, the initial conditions obtained from the Launch Vehicle provider according the worst condition of separation are represented by angular velocities  $\omega = [4 \quad 4 \quad 2]^T \text{ deg/s}$ , attitude in Euler Angles  $EA = [40 \quad 40 \quad 40]^T \text{ deg}$ , pitch wheel bias  $h = [0 \quad -0.1 \quad 0]^T \text{ N.m.s}$ , position  $R_S = [-1220 \quad -966.5 \quad 6854]^T \text{ km}$ , and velocity  $V_S = [-7.426 \quad 0.1801 \quad -1.277]^T \text{ km/s}$ . For the MSDRE controller, two sets of weighting matrices  $R$  and  $Q$  are used for the both flight modes, while the switching occurs according to value of the angular velocity and

scheduled such that  $R = [10^8 \ 10^8 \ 10^8]^T$  and  $Q = \text{diag} \left[ \begin{matrix} 2.0 \times 10^8 & 2.0 \times 10^8 & 2.0 \times 10^8 \\ 10^6 & 10^6 & 10^6 & 1.0 \end{matrix} \right]^T$  for detumbling mode while for stabilization mode  $R = [10^8 \ 10^8 \ 10^8]^T$  and  $Q = \text{diag} \left[ \begin{matrix} 2.0 \times 10^8 & 4.0 \times 10^9 & 2.0 \times 10^8 \\ 5.5 \times 10^6 & 5.5 \times 10^6 & 5.5 \times 10^6 & 1.0 \end{matrix} \right]^T$ . The switching condition is represented by  $\omega_x^{bo} \leq 0.03 \text{ deg/s}$  and  $\omega_z^{bo} \leq 0.03 \text{ deg/s}$ . The three-axis magnetometer (TAM) sensor noise has a standard deviation  $\sigma_B = 50 \text{ nT}$ . The induced noise due to measurement differentiation can be calculated as  $v_{B_k} = \frac{v_{B_{k+1}} - v_{B_k}}{\Delta t}$ . So, it is also a zero mean white noise with a standard deviation  $\sigma_B^2 = \frac{2\sigma_B^2}{\Delta t}$ . The sampling time of the ADCS control loop is larger than the sampling time of the magnetometer which is considered a fast sensor. So, during one sampling interval, several magnetometer readings can be obtained. Then, the time derivatives of the magnetic field measurements are computed in a semi analytical method via differentiating the polynomials result from a cubic spline fit of the measurement data during each sampling interval. Care must be taken to use a reasonable number of readings during the sampling interval since using a low number, results in poor presentation of the magnetic field and a high number results in very noisy derivatives. To preserve the quaternion normalization constraint, different methods handled this problem such as adding a pseudo – measurement or truncating the state vector. For simplicity and reduction of the computational burden, quaternion normalization; namely  $q_{k+1/k+1}^* = \frac{\hat{q}_{k+1/k+1}}{\|\hat{q}_{k+1/k+1}\|}$  is used through this work. The filter is initialized using initial states

$$x_0 = [0 \ 0 \ 0 \ 0 \ 0 \ 0 \ 1.0 \ 0 \ 0 \ 0 \ 0]^T \quad \text{and} \\ P_{f_0} = \text{diag} \left[ \begin{matrix} [0.2094^2 & 0.2094^2 & 0.2094^2]^T \\ [1_{1 \times 4}]^T \\ [0.05^2 & 0.05^2 & 0.05^2]^T \\ 0.01^2 \end{matrix} \right]$$

as initial error covariance while, the process and measurement noise covariance matrices  $Q_f$  and  $R_f$  are assembled according to

$$Q_f = \text{diag} \left[ \begin{matrix} [(6.25 \times 10^{-7})^2 & (5.99 \times 10^{-7})^2 & (7.04 \times 10^{-7})^2]^T \\ [0_{1 \times 4}]^T \\ [(10^{-5})^2 & (10^{-5})^2 & (10^{-5})^2]^T \\ 0.01^2 \end{matrix} \right] \\ R_f = \text{diag} \left[ \begin{matrix} [(5.0 \times 10^{-8})^2 & (5.0 \times 10^{-8})^2 & (5.0 \times 10^{-8})^2]^T \\ [(6.25 \times 10^{-9})^2 & (6.25 \times 10^{-9})^2 & (6.25 \times 10^{-9})^2]^T \end{matrix} \right]$$

The rest of the simulation parameters are defined to be magnetorquer strength  $M_{max} = [10 \ 10 \ 10]^T \text{ A.m}^2$ , spacecraft dipole  $m = [0.3 \ 0.3 \ 0.3]^T \text{ A.m}^2$ , drag coefficient  $C_d = 2$ , time Span of 20 orbit, and sampling time of 4 s. The integration algorithm used for the

modified Riccati equation and state propagation is Runge - Kutta ode4 and the magnetic field vector  $B$  is based on IGRF 2005 Model. Figure 4 indicates the minor influence of the matrix  $\Gamma(x)$  in Eq. (42) compared to  $A(x)$  and is since the resulting r.m.s error of the angular velocity is less than  $0.002 \text{ deg/s}$  and almost zero for the quaternion. The total angular velocity is depressed after separation from  $6 \text{ deg/sec}$  to  $0.072 \text{ deg/sec}$  in 1.5 orbit and kept to less than  $0.03 \text{ deg/sec}$  upto 20 orbits as shown in Fig. 5. The pointing and angular velocity errors are shown in Figs. 6 and 7 through two time windows. The first one represents the detumbling mode and extends upto 3 orbit and the other shows the performance during the standby mode. The MSDRE controller successfully drives the spacecraft from detumbling mode to become in an Earth pointing mode in less than two orbits since the pointing error starts to be bounded within  $5 \text{ degs}$  and the angular velocity error reaches values less than  $0.05 \text{ deg/sec}$ . Then these conditions are maintained during the standby mode as shown in the right hand side of Figs. 6 and 7. Figure 8 gives a picture of the history of the applied dipole moments, and the corresponding control torque appears in Fig.9. It should be mentioned here that the hardware configuration and sizing are kept to the original values as in EgyptSat-1, since the magnetorquers in addition to the reaction wheels are utilized to control the spacecraft while in the current work only magnetorquers are used. However, larger values of the dipole moments might be used to avoid reaching the saturation limits specially, during the standby mode. The stability condition in Eq. (53) is verified as in Fig. 10 which indicates the history of the Lyapunov function and its time derivatives through all over the both modes. Figures 11 through 14 describe the performance of the proposed filter. The first two figures show the fast convergence of the filter since it successfully estimated the attitude and rate within the required values. It clearly can be shown the synchronization of the convergence of the filter and the controller, since the filter also, starts to reach the required accuracy for the attitude and rate in less than two orbits and kept this accuracy throughout the standby mode to be better than  $5 \text{ degs}$  and less than  $0.03 \text{ deg/sec}$  for the attitude and rate respectively. Figures 13 and 14 indicate the estimation errors for the spacecraft dipole and the drag coefficient. Both parameters start to converge almost after 6 orbits to reach steady state values of  $0.02 \text{ A.m}^2$  and  $0.13$  for the spacecraft dipole and the drag coefficient respectively. Finally to estimate the stability regions of the candidate MSDRE controller, uniformly random distributed initial conditions on the intervals  $[-150 \ 150] \text{ deg}$  and  $[-5 \ 5] \text{ deg/s}$  for each axis are generated and stability condition in Eq. (53) is investigated also, the attitude and rate estimation accuracy are investigated throughout the same intervals to demonstrate filter convergence and



stability. Figures 15 and 16 give the resulting stability regimes for the overall ADCS.

### 7 Conclusions

A modified state-dependent Riccati equation MSDRE based controller has been developed and adopted for spacecraft attitude maneuver/tracking. An extended Kalman filter EKF based estimator has been developed for attitude and rate estimation using only one reference sensor. While the magnetometer measurements are used through this paper, any other reference sensor can be used or added to the measurement model. The stability of the controller and estimator is demonstrated by identifying the regimes of different initial conditions which lead to Lyapunov function convergence and bounded attitude and rate estimation accuracy.

#### Acknowledgments

This work is supported by the Korean Science and Engineering Foundation (KOSEF) through the National Research Laboratory Program funded by the Ministry of Science and Technology (No. M10600000282-06j0000-28210).

#### References:

[1] Lefferts, F. Markley, and M. Shuster, "Kalman Filtering for Spacecraft Attitude Estimation," *Journal of Guidance, Control, and Dynamics*, Vol. 5, No. 5, Sept.-Oct. 1982, pp. 417-429.  
 [2] B. Anderson, and J. Moore, *Optimal Control*, Prentice-Hall, Inc., A Division of Simon & Schuster, Englewood Cliffs, NJ 07632, 1989.  
 [3] R. Wisniewski, "Linear Time Varying Approach to Satellite Attitude Control Using Only Electromagnetic Actuation," *Journal of Guidance, Control, and Dynamics*, Vol. 23, No. 4, 2000, pp. 640-647.  
 [4] M. L. Psiaki, "Magnetic Torquer Attitude Control via Asymptotic Periodic Linear Quadratic Regulation," *Journal of Guidance, Control, and Dynamics*, Vol. 24, No. 2, 2001, pp. 386-394.  
 [5] J. R. Cloutier, and D. T. Stansbery, "The Capabilities and Art of State-Dependent Riccati Equation-Based Design," *Proceedings of the American Control Conference*, Anchorage, Alaska, May 2002.  
 [6] W. Luo and Y. -C. Chu, "Attitude Control Using the SDRE Technique," *Seventh International Conference on Control, Automation, Robotics and Vision*, Singapore, December 2002.  
 [7] M. Abdelrahman, and S-Y Park "Simultaneous Spacecraft Attitude and Orbit Estimation Using Magnetic Field Vector Measurements," *Proceedings of the 7th ESA Conference on Guidance, Navigation & Control Systems*, 2-5 June 2008, Tralee, Ireland.

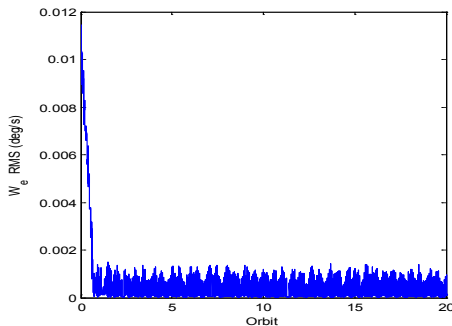


Fig 4 Effect of  $\Gamma$  Matrix on the Spacecraft Dynamics

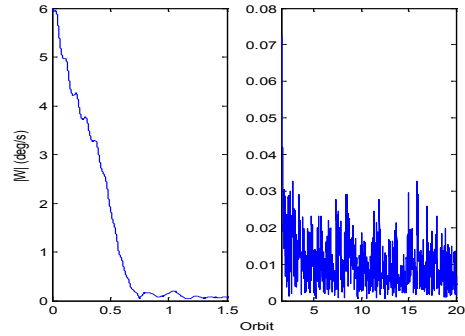


Fig. 5 Total Angular Velocity History (Detumbling –Transient/Standby)

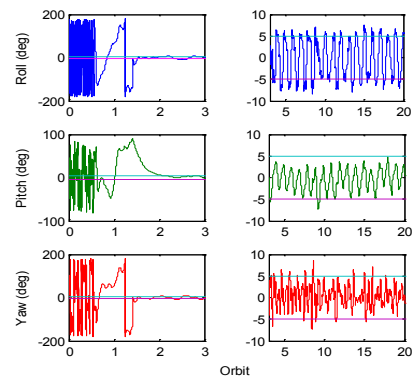


Fig. 6 Pointing Error (Detumbling/Transient-Standby)

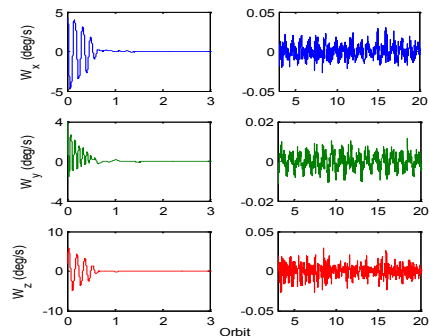


Fig. 7 Angular Velocity Error (Detumbling/Transient-Standby)

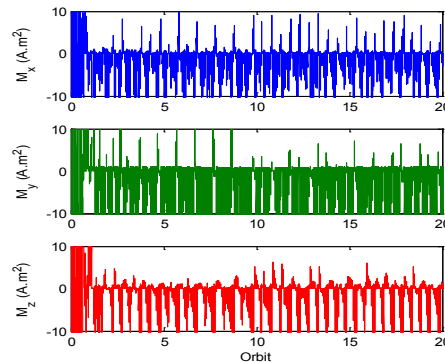


Fig. 8 Applied Dipole Moments

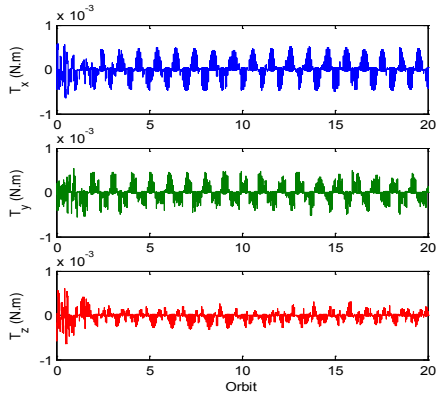


Fig. 9 Applied Control Torque

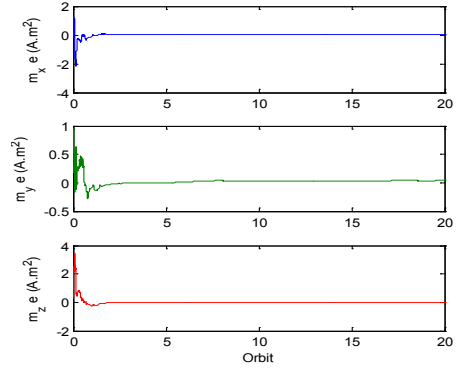


Fig. 13 Spacecraft Dipole Estimation Error

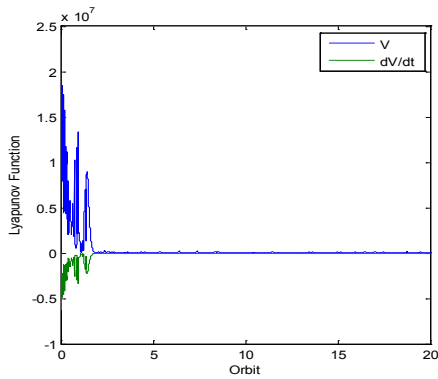


Fig.10 Lyapunov Function and Its Time Derivative

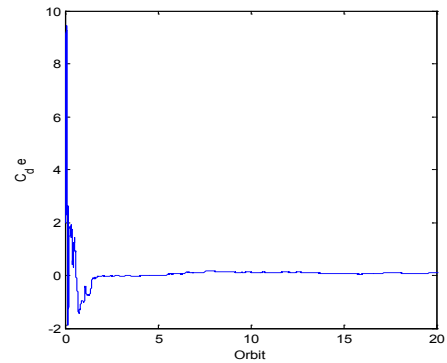


Fig. 14 Drag Coefficient Estimation Error

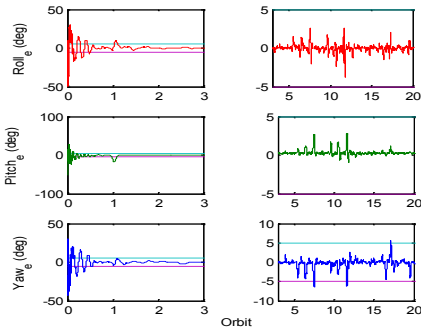


Fig. 11 attitude Estimation Error (Detumbling/Transient-Standby)

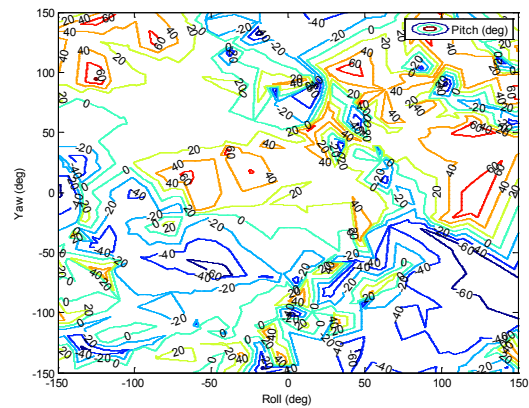


Fig.15 Euler Angles Stability Regimes

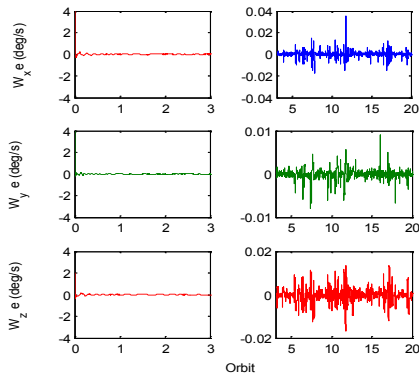


Fig. 12 Angular Velocity Estimation Error (Detumbling/Transient-Standby)

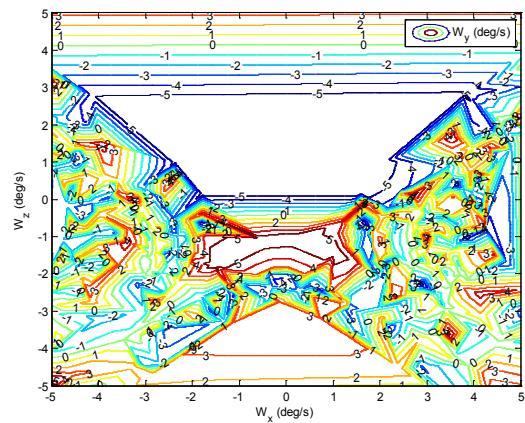


Fig. 16 Angular Velocity Stability Regimes